Laser-Induced Deposition of Palladium and Gas-Phase Photofragmentation Pathways from (2-Methylallyl)(1,1,1,5,5,5-hexafluoro-2,4-pentanedionato) Palladium

Jinwoo Cheon,† Peter Muraoka, and Jeffrey I. Zink*

Department of Chemistry and Biochemistry, University of California—Los Angeles, Los Angeles, California 90095

Received September 1, 1999. Revised Manuscript Received November 10, 1999

Metallic palladium films are prepared at 10^{-2} Torr by 308 nm irradiation of gaseous (2-methylallyl)(1,1,1,5,5,5-hexafluoro-2,4-pentanedionato) palladium. Gas-phase luminescence spectra recorded during the photochemical deposition process are used to identify photofragments. X-ray photoelectron analysis of the films shows that they consist primarily of palladium metal; the films produced with H_2 carrier gas have no detectable fluorine and barely discernible carbon contaminants. The Pd films are polycrystalline fcc (face-centered cubic) palladium with preferential growth along the 111 direction. Scanning electron microscopy shows that the films formed with H_2 carrier gas are smooth and consist of granules less than 35 nm in diameter. Further characterization of the gas-phase photofragmentation process is carried out by time-of-flight mass spectroscopy. The dominant peak present in the mass spectrum under 308 nm irradiation arises from palladium ions. No fragments containing palladium and other elements (especially PdC or PdF) are found. Pathways of photofragmentation, comparisons with other metal 1,1,1,5,5,5-hexafluoro-2-4-pentanedionate compounds, and the implications for laser-assisted chemical vapor deposition are discussed.

Laser-assisted metal organic chemical vapor deposition (LCVD) relies on the use of volatile organometallic compounds to deliver material to a photolysis chamber where the compound is photodecomposed (by photochemical reactions or local heating at the laser spot), leaving behind the material to be deposited (and possibly undesired contaminants).[1] Advantages of LCVD include spatially selective deposition on the substrate, selective energy transfer to the deposition precursor, and low processing temperatures.[2−10] Efforts to fabricate multilayer structures with well-defined physical properties and abrupt interfaces benefit from the low growth temperatures.[1,11] Pd metal films have potential applications as catalysts and as electrical contacts in microelectronics. Pyrolytic metal organic CVD studies of palladium complexes with hfac (1,1,1,5,5,5-hexafluoro-2−4-pentanedionate) and allyl ligands have been reported.[12−17]

Recent studies of the luminescence that is observed when metal-containing molecules are photolyzed under photochemically driven CVD conditions have shown that diatomic metal-containing molecules and metal atoms are produced in the gas phase.[18−24] These discoveries have assisted in the elucidation of the photolytic decomposition pathways. Both desired (e.g., TiN in the laser CVD of TiN films)[24] and undesirable fragments containing heteroatoms that contaminate the final films

† Current address: Center for Molecular Science and Department of Chemistry, Korea Advanced Institute of Science and Technology (KAIST), Taejon 305-701, Korea.

(1) For reviews, see: (a) Eden, J. G. *Photochemical Vapor Deposition*; Wiley: New York, 1992. (b) Hitchman, M. L.; Jensen, K. F. *Chemical Vapor Deposition: Principles and Applications*; Academic Press: San Diego, 1993. (c) Kodas, T. T.; Hampden-Smith, M. J. *The Chemistry of Metal CVD*; VCH: Weinheim, 1994.
(2) Avey, A. A.; Hill, R. H. *J. Am. Chem. Soc.* **1996**, *118*, 237.
(3) Larciprete, R. *Appl. Surf. Sci.* **1990**, *46*, 19.
(4) Doppelt, P.; Baum, T. H. *MRS Bull.* **1994**, *19*, 41.
(5) Lee, E. J. B.; T. W.; Ha, J. S.; Shane, M. J.; Sailor, H. J. *J. Am. Chem. Soc.* **1996**, *118*, 5375.
(6) Bhatia, S. K.; Hickman, J. J.; Ligler, F. S. *J. Am. Chem. Soc.* **1992**, *114*, 4432.
(7) Dressick, W. J.; Dulcey, C. S.; Georger, J. H.; Calvert, J. M. *Chem. Mater.* **1993**, *5*, 148.
(8) Moreau, W. M. *Semiconductor Lithography: Principles, Practices, and Materials*; Plenum: New York, 1988.
(9) Kompa, K. L. *Angew. Chem., Int. Ed. Engl.* **1988**, *27*, 1314.
(10) Baum, T. H., Commita, P. B. *Thin Solid Films* **1994**, *80*, 218.
(11) Herman, I. P. *Chem. Rev.* **1989**, *89*, 1323.
(12) Gozum, J. E.; Pollina, D. M.; Jensen, J. A.; Girolami, G. S. *J. Am. Chem. Soc.* **1988**, *110*, 2688.
(13) Lin, W.; Warren, T. H.; Nuzzo, R. G.; Girolami, G. S. *J. Am. Chem. Soc.* **1993**, *115*, 11644.
(14) Feurer, E. Suhr, H. *Thin Solid Films* **1988**, *81*, 137.
(15) Yuan, Z.; Puddephatt, R. J. *Adv. Mater.* **1994**, *6*, 51.
(16) Zhang, Y.; Yuan, Z.; Puddephatt, R. J. *Chem. Mater* **1998,** *10*, *2293*.
(17) Hierso, J.-C.; Satto, C. Feurer, R.; Kalck, P. *Chem. Mater.* **1996**, *8*, 2481.
(18) Wexler, D.; Zink, J. I.; Tutt, L.; Lunt, S. R. J. *Phys. Chem.* **1993**, *97*, 13563.
(19) Talaga, D. S.; Zink J. I. *Inorg. Chem.* **1996**, *35*, 5050.
(20) Cheon, J.; Talaga, D. S.; Zink, J. I. *J. Am. Chem. Soc.* **1997**, *119*, 163.
(21) Cheon, J.; Zink, J. I. J. *Am. Chem. Soc.* **1997**, *119*, 3838.
(22) Cheon, J.; Zink, J. I. *Chem. Mater.* **1997**, *9*, 1208.
(23) Talaga, D. S.; Hanna, S. D.; Zink J. I. *Inorg. Chem.* **1998**, *37*, 2880.
(24) Cheon, J.; Guile, M.; Muraoka, P.; Zink, J. I. *Inorg. Chem.* **1999**, *38*, 2238.

10.1021/cm990566q CCC: $19.00
Published on Web 00/00/0000 PAGE EST: 5.2

(e.g., CuF, CrF, NiF, PtC, and PdC in the laser CVD of the respective metal films)[19−23] have been identified. The fluorinated acetylacetonate ligands (hfac) that were used in the latter studies provide good precursor volatility and allow for facile transport in the gas phase, but they may also result in fluorine or carbon contamination of the final deposit.[25]

In our prior work on metal−hfac complexes, we proposed two mechanisms by which diatomic metal fluoride or metal carbide molecules could be produced; one was based on η^1 bonding of the hfac ligand to the metal by its central carbon.[19,23] This type of bonding has been shown to exist in platinum hfac complexes.[26] Luminescence spectroscopic studies of $Pt(hfac)_2$ under LCVD conditions showed that diatomic PtC was produced in the gas phase. We have recently expanded the detection methods by using time-of-flight (TOF) mass spectroscopy; these studies showed that PdC is formed during the gas-phase photolysis of $Pd(hfac)_2$. Mass spectroscopy is useful because it detects the ionic species that are produced by photolysis (including both the primary ionic photoproducts and secondary ions that are produced by photoionization of the neutral primary photoproducts by additional photons.) The mass spectroscopic measurements complement the luminescence studies; the latter detect all species (both ionic *and* neutral) that emit.

In this paper, we report the laser-assisted CVD of palladium films from (2-methylallyl)(1,1,1,5,5,5-hexafluoro-2,4-pentanedionato) palladium, (2-Me-allyl)(hfac)-Pd. The properties of the films are characterized by X-ray diffraction, X-ray photoelectron spectroscopy, and scanning electron microscopy. Luminescence spectroscopy and mass spectroscopy are used to identify the gas-phase photoproducts. The photofragmentation patterns that are observed for (2-Me-allyl)(hfac)Pd provide insight into the final film quality. The role of the weakly bonded allyl ligand in the photofragmentation process is also discussed.

Experimental Section

(2-methylallyl)(1,1,1,5,5,5-hexafluoro-2,4-pentanedionato) palladium was prepared by a modification of a literature method in which bis(methylallyl)di-μ-chlorodipalladium, $[Pd(2\text{-methylallyl})Cl]_2$ is reacted with the sodium salt of hexafluoroacetylacetonate.[27] The compound is obtained as pale yellow needles that are volatile and sublime at about 40 °C under vacuum (10^{-2} Torr). After purification by sublimation and characterization by NMR (^1H and ^{19}F) and mass spectroscopy (EI, electron ionization), they were used for the CVD and gas-phase experiments.

The thin film photodeposits were characterized by surface analytical methods. X-ray powder diffraction (XRD) patterns were acquired using Cu Kα radiation with a power supply of 40 kV and 30 mA. Scanning electron micrographs were obtained on a Cambridge Stereo Scan 250 instrument. X-ray photoelectron spectra were obtained with a 15 kV and 400 W Al Kα radiation source (1486.6 eV) at a pressure of ca. 10^{-9} Torr. The surfaces of the films were cleaned by Ar^+ sputtering for 3−5 min (corresponding to roughly 20−30 nm in depth).

Luminescence Spectroscopy Luminescence experiments were carried out in an evacuated stainless steel six-way cross with synthetic fused silica windows. A sample of the precursor was placed in the sample chamber and was leaked into the photolysis chamber with a needle valve. The gas-phase luminescence spectra were obtained by exciting the gas-phase sample with 308 nm radiation from a XeCl excimer laser (Lambda Physik EMG 201 MSC) under vacuum produced by continuous pumping (10^{-2} Torr). The pulse energy used for excitation of the CVD precursors is approximately 3 mJ, and the resulting fluence is typically ~3 MW/cm^2. The focused output of the laser excites the gaseous sample, and the emitted light is collected at right angles and directed into a 0.32 m single monochromator (JY HR320), where it is dispersed by a 300 or a 600 groove/mm holographic grating and detected by an UV-intensified diode array detector (EG&G Princeton Applied Research OMA3 1024 × 1). Details of this experimental setup are described elsewhere.[19,21]

Time-of-Flight Mass Spectroscopy. The TOF mass spectrometer was constructed at UCLA. The precursor is admitted to the high-vacuum chamber via a supersonic jet. The base pressure of the chamber is less than 10^{-6} Torr. The photoionization for mass spectroscopy is carried out in a stainless steel cube (30 cm edge length) with quartz windows evacuated to 10^{-6} Torr with a 12 in. diffusion pump fitted with a water-cooled baffle. A General Valve series 9 high-speed solenoid valve (0.5 mm orifice) sends a 0.2 ms pulse of the sublimed sample downward to intersect the incoming photons at 90°. A XeCl excimer laser (Lambda Physik EMG 201 MSC) provides 308 nm photons required for photolysis. Once the fragment ions are produced, they are accelerated down a 1m flight tube by a series of three stainless steel plates that have stainless steel mesh across an open center. Acceleration plate voltages are 3000 V, 2100 V, and ground, respectively in order from furthest to nearest the detector. The flight tube is kept at 10^{-6} Torr using a Varian V300HT 6 in. air-cooled turbomolecular pump, and ions are detected using an 18 mm microchannel plate detector assembly. The detector assembly is fitted with two Galileo MCP 18B plates with a 10 μm channel diameter and a channel spacing of 12.5 μm. The ion current is processed using a computer-controlled RTD710 Tektronix 200 MHz dual-channel digitizer.

Results

1. Photodeposition. Laser-driven CVD was carried out at 3×10^{-1} Torr using a XeCl excimer laser (308 nm, 20 Hz) as the excitation source. The palladium precursor was heated in a reservoir cell to its sublimation temperature (55 °C) and was leaked into a stainless steel six-way cross with quartz windows. All of the experiments were carried out under dynamic vacuum (constant pumping) conditions with either the pure precursor or the addition of hydrogen gas**.** The laser beam was focused to a rectangular spot with dimensions of about 1 × 2 cm^2 with a fluence at the substrate of about 1 MW/cm^2. Both quartz and Si (100) substrates at room temperature were used. The resulting deposits were nonreflecting black when the pure precursor was used or shiny when the H_2 carrier gas was used. The deposits did not adhere strongly to either substrate. Final film thicknesses after about 2 h of irradiation were 0.1 μm. No attempts were made to optimize the deposition rates.

The deposits were examined by using scanning electron microscopy. The films formed with H_2 as the carrier gas were smooth; close examination revealed that they consisted of very small granules less than 35 nm across (Figure 1a). EDS analysis of the film produced with the H_2 carrier gas showed the presence of palladium and silicon (from the substrate). Deposits formed without a carrier gas were granular with grain sizes about 150 nm (Figure 1b).

(25) Shulz, D. L.; Marks, T. J. *Adv. Mater* **1994**, *6*, 719.
(26) Lewis, F. D.; Miller, A. M.; Salvi, G. D. *Inorg. Chem.* **1995**, *34*, 3173.
(27) Tatsuno, Y.; Yoshida, T.; Otsuka, S. *Inorg. Synth.* **1979**, *19*, 220.

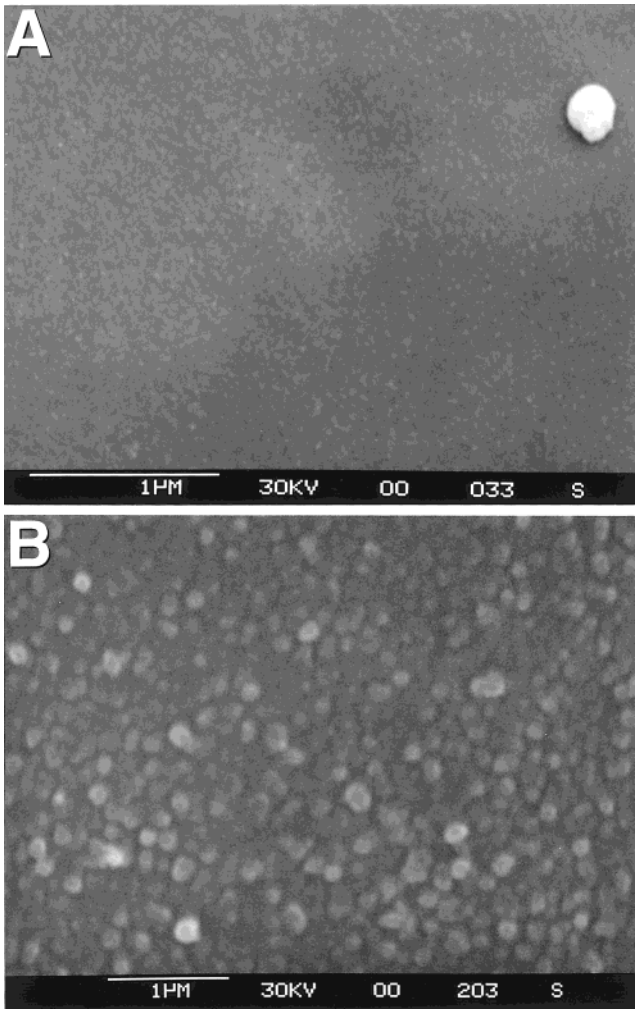

Figure 1. Scanning electron microscopy images of palladium films grown by LCVD. The photographs show the films that are formed when H_2 is used as the carrier gas (top) and without a carrier gas (bottom).

X-ray photoelectron spectroscopy was carried out to examine the elemental composition of the films. The films produced with no carrier gas consisted primarily of palladium metal with carbon and fluorine contaminants (Figure 2, top). The films produced with H_2 carrier gas consisted of purer palladium metal (Figure 2, bottom). The relative intensities of both the carbon and fluorine peaks decreased after argon ion sputtering with the fluorine peak decreasing to below the level of the noise and the carbon peak remaining barely discernible.

X-ray diffraction of the films showed that they consisted of polycrystalline fcc (face-centered cubic) palladium with preferential growth along the 111 direction. The 111, 200, 220, 311, and 222 peaks were observed at 2θ of 40.1, 46.6, 68, 82, and 86.6°, respectively.[28] No peaks from PdC, PdF_2, or PdF_3 were found. These results suggest that the carbon and fluorine found by the XPS analysis results from interstitial contamination and not from compound formation. These observations are consistent with the photofragmentation studies discussed later.

2. Gas-Phase Optical Spectroscopy. Strong yellow visible luminescence is easily observed during the laser

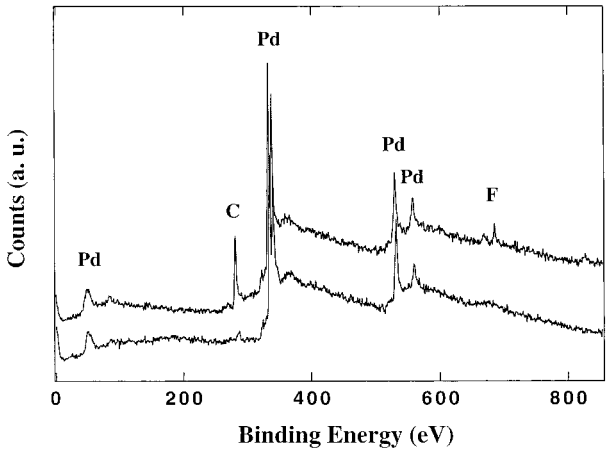

Figure 2. X-ray photoelectron spectra of palladium films grown by LCVD with no carrier gas (top) and with H_2 as the carrier gas (bottom). Both spectra are obtained after argon ion sputtering.

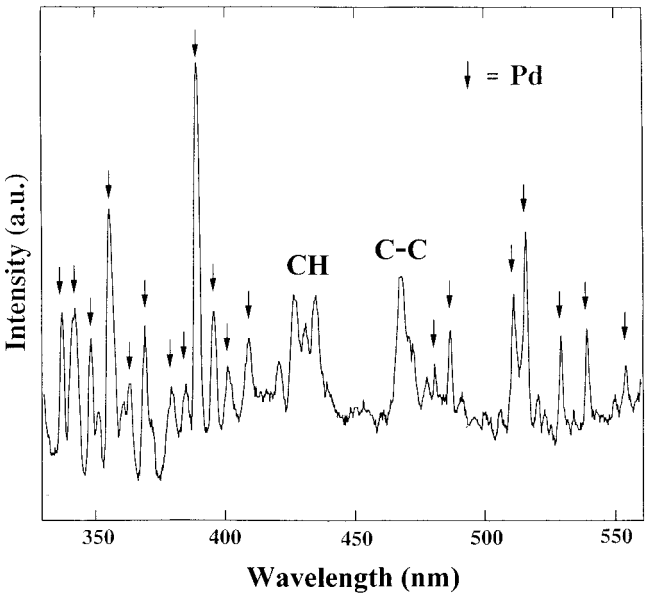

Figure 3. Luminescence spectra obtained by exciting (2-Me-allyl)(hfac)Pd at 308 nm under the conditions used for LCVD ($\sim 10^{-2}$ Torr). The peaks marked with arrows are emission lines from atomic palladium. Peaks arising from CH and CC emissions are labeled.

CVD experiments under dynamic pumping. To identify the emitting species, luminescence spectra were taken under the CVD conditions. The emission spectrum in the wavelength range between 330 and 560 nm is shown in Figure 3. The spectrum is dominated by a large number of atomic emission lines from palladium atoms. The strongest atomic palladium emission lines occur at 337.1, 342.1, 348.4, 355.5, 389.1, 395.5, 401.0, 510.9, and 515.9 nm.[29,30] Other strong emission lines originate from CH (origin at 431 nm) and C_2 (broad peak at 467−473 nm) diatomics.[31]

The solution absorption spectrum of the compound is dominated by a peak in the near-ultraviolet at 320 nm

(28) *JCPDS Powder Diffraction File*; McClune, W. F., Ed.; International Center for Diffraction Data: Swarthmore, PA, 1990.

(29) Weise, W. L.; Martin, G. A. *Wavelength Transition Probabilities for Atoms and Atomic Ions*; U. S. Gov. Printing Office: Washington, DC, 1980.

(30) Striganov, R.; Sventitskii, N. S. *Tables of Spectral Lines of Neutral and Ionized Atoms*; IFI/Plenum: New York, 1968.

(31) Pearse, R. W. B.; Gaydon, A. G. *The Identification of Molecular Spectra*, 3rd ed.; Chapman and Hall: London, 1976.

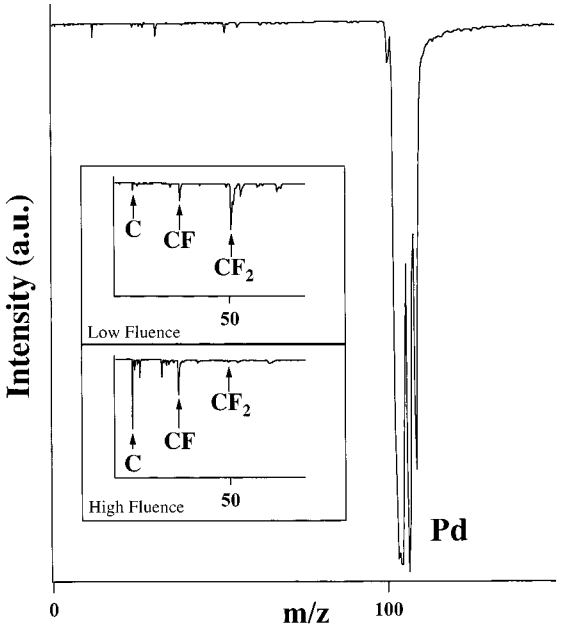

Figure 4. Time-of-flight mass spectra produced when (2-Me-allyl)(hfac)Pd is excited by 308 nm laser pulses. The spectrum is dominated by the isotopes of palladium ions. The insert shows a magnification of the lower mass region as the laser fluence is increased (top to bottom).

($\epsilon = 1.1 \times 10^4$ M^{-1} cm^{-1}). A $\pi\pi^*$ transition centered on the acetylacetonate ligand is known to give rise to a strong absorption band in this region,[32] but the spectrum of the molecule has not been assigned. The 308 nm excitation wavelength is slightly to the high-energy side of the peak, whereas the 355 nm excitation is at the low-energy edge of the band. No obvious luminescence was observed when the compound was studied at 15 K in a glass or as a powder. No luminescence from the free hfac ligand was observed in the gas-phase experiments.

3. Mass Spectroscopic Identification of Photofragments. Intramolecular photofragmentation was studied under the collision-free environment of a molecular beam by using time-of-flight mass spectroscopy. The mass spectra, shown in Figure 4, reveal that extensive fragmentation takes place in one laser pulse. The spectrum is dominated by palladium ions (Figure 4); the intensity of the next biggest peak is less than 1/100th that of palladium.

Magnification of the nonpalladium peaks reveals two important results that will play a major role in the following discussion: there are no fragments that contain both palladium and other atoms, and the hfac ligand itself is extensively fragmented (Figure 4 inset). The former is important because studies on other metal complexes showed that diatomic metal fluorides and carbides are common.[19−23] A careful search of the appropriate regions of the spectra failed to reveal peaks from PdF or PdC. The second result is important because it has direct implications for the origins of the impurities in the films. The heaviest mass fragment of the hfac ligand is CF_3CO, $m/z = 97$. CF_3, CF_2, CF, and C are also observed (Figure 4).

The laser pulse energy strongly affects the intensity distributions of the carbon-containing fragments. As the fluence is increased, the intensities of the smallest fragments increases relative to those of the larger masses. The inset to Figure 4 shows mass spectra taken at the highest and lowest fluences used in this study. In these spectra, at the highest fluence, the peak arising from C^+ is larger than those arising from CF_n^+ species, but as the fluence is decreased, the relative intensities change and heavier mass fragments become more prominent. Under all of the conditions studied in this work, however, the intensity of the palladium peak is 2 orders of magnitude larger than that the next largest peak.

Discussion

1. Properties of the Deposit. Gas-phase photolysis of (2-Me-allyl)(hfac)Pd causes deposition of polycrystalline palladium metal on silicon and silica substrates. The identity of the films is confirmed by XRD (only reflections characteristic of palladium are observed), EDS, and XPS. The latter analysis shows that the films contain carbon and fluorine impurities. Argon ion sputtering of the films produced by using H_2 as the carrier gas shows that the fluorine and most of the carbon (probably amorphous) are surface contaminants.

The highest purity films are those grown with H_2 as the carrier gas. CVD studies involving pyrolysis under H_2 atmospheres have shown that the purity of metal deposits is improved.[1c] Many of the photoproduced fragments that are observed in the mass spectrum are reactive species that will react with hydrogen to produce more stable and less reactive compounds. The H_2 carrier gas in the CVD experiments has a much higher concentration than the relatively low-vapor-pressure precursor. Multiple collisions between hydrogen and the reactive carbon- and fluorine-containing fragments will produce saturated species that are much less reactive with palladium atoms and the surface than are the reactive ions and radicals initially produced by the laser pulse.

2. Emission Spectroscopy. During the course of the laser-assisted CVD studies, a bright yellow luminescence in the path of the laser beam in the cell is observed. The luminescence provides the opportunity to identify excited photochemical species that are formed during the CVD process and to use the information to develop an understanding of the photofragmentation pathways. The luminescence spectrum that is recorded during the deposition process is shown in Figure 3. It exhibits a large number of relatively sharp lines. Those indicated with arrows are atomic emission lines from neutral palladium atoms.

The emission spectra show that the luminescence originates primarily from gas-phase photofragments and not from the intact precursor molecule. Metal atom emission caused by pulsed laser irradiation of volatile metal complexes is common.[35] This result is not surprising because the metal−ligand bonds are frequently the

(32) Wexler, D.; Zink, J. I. *Inorg. Chem.* **1996**, *35*, 4064.

(33) Izquierdo, R.; Bertomeu, J.; Suys, M.; Sacher, E.; Meunier, M. *Appl. Surf. Sci.* **1995**, *86*, 509.

(34) *Laser Chemical Processing for Microelectronics*; Ibbs, K. G., Osgood, R. M., Eds.; Cambridge University: Cambridge, 1989.

(35) *Laser Chemistry of Organometallics*; Chaiken, J. Ed.; ACS Symposium Series, American Chemical Society: Washington, DC, 1993.

weakest bonds in the metal complex and photodissociation of the ligands is a facile photochemical process. The presence of emission bands from fragments of the ligands such as CH and C_2 show that multiphoton fragmentation is occurring. Photoinitiated metal−ligand bond breaking followed by photon absorption by the free ligands and further fragmentation is well-known in a variety of metal complexes.[36,37]

The identification of palladium atoms by emission spectroscopy is complementary to the identification of photoproduced ions by using time-of-flight mass spectroscopy. Emission spectroscopy can be used to identify all of the gas-phase species that emit, including neutral palladium atoms and CH and C_2 molecules, whereas mass spectroscopy can be used to identify ions. Comparisons of photofragments identified by both methods is rare, but progress is being made. For example, the important metal nitride diatomic fragments produced by photolysis of metal amide complexes were recently characterized by both luminescence spectroscopy (neutral TiN and ZrN) and mass spectroscopy (TiN^+ and ZrN^+).[24] In the case of diatomic fragments containing palladium such as PdF or PdC that could lead to contamination of the LCVD-produced films, cross comparisons cannot easily be made because luminescence of these fragments has not been reported and their presence or absence must be determined by mass spectroscopy.

3. Photofragmentation Processes and Film Content. The photofragmentation patterns observed for (2-Me-allyl)(hfac)Pd provide results that give insight into the final film quality. The most important issues are the origins of the fluorine and carbon contaminants in the photodeposit.

Absence of PdF and PdC. Previous studies on metal hfac complexes have shown that diatomic metal fluorides are produced by an intramolecular reaction in the gas phase. CrF, NiF, and CuF were observed in the emission during photofragmentation of $Cr(hfac)_3$, $Ni(hfac)_2$, and $Cu(hfac)_2$, respectively.[23] Similarly, emission during photofragmentation of $Pt(hfac)_2$ proved that PtC is formed by an intramolecular process.[23] Emission spectra of PdF and PdC have not been reported; in the absence of known bands from these species, we cannot make any claims about the presence or absence of PdF or PdC based only on our emission spectra during photofragmentation of (2-Me-allyl)(hfac)Pd.

Neither PdF^+ nor PdC^+ are present in the photofragmentation mass spectra of (2-Me-allyl)(hfac)Pd. In contrast, the mass spectrum of $Pd(hfac)_2$ shows that PdC^+ is produced during photofragmentation. In both of these compounds, the Pd^+ ion peak dominates the mass spectrum, but the PdC^+ peak that is clearly present in the spectrum from the bis(hfac) complex is absent in that from (2-Me-allyl)(hfac)Pd.

The absence of PdC in the photolysis products of (2-Me-allyl)(hfac)Pd and its presence in those of $Pd(hfac)_2$ provides insight into the mechanisms. The 2-Me-allyl-Pd bond is weak compared to the hfac−Pd bonds. Thus, it may be possible that one photon contains enough energy to dissociate both the allyl and the hfac ligands, and fluorine or carbon atom abstraction by the palladium does not occur. In contrast, in the bis(hfac) complex, the first photon may only cause dissociation of one of the ligands; either the residual energy in the Pd−hfac fragment is enough to cause atom abstraction or else another photon is absorbed and abstraction occurs. (In the case of the bis(hfac) platinum complex, PtC formation was reported to obey a two-photon power law.[23]) These results suggest that the presence of a weakly bonded ligand may enhance complete ligand dissociation and suppress atom abstraction. Further studies of metal complexes containing the hfac ligand and a second weakly bonded ligand are in progress.

Photofragments Containing Fluorine and Carbon. Fluorine and carbon contamination of the film probably arises from fragmentation of a free hfac ligand after it has dissociated from the metal. The pulse energy dependence of the fragmentation supports this suggestion. The production of the bare palladium metal follows an observed one-photon power law. (If saturation effects occur, this experimental one-photon power dependence may be misleading and multiphoton fragmentation and ionization may be occurring.) At the lowest pulse energies that were studied, the palladium ion peak dominates the mass spectrum and the next largest peak is less than one-hundredth as intense (Figure 4). Complete ligand dissociation has occurred, but ionization of the free hfac ligand has not. As the pulse energy is increased, the free ligand absorbs and fragments, and fluorine-containing fragments appear. The observed power law for these fragments involves more photons than that for the palladium metal, and the power dependencies of the fluorine-containing fragments differ among themselves.

The behavior of the carbon- and fluorine-fragment intensities in the mass spectrum is interesting. The trends can be observed in the inset to Figure 4. At the lowest pulse energies (near the ion detection threshold), the peak from C^+ is just above the signal-to-noise level, and the intensities follow the order $C^+ < CF^+ < CF_2^+$. At the highest fluences, the C^+ peak is the largest, and the order is reversed. These trends probably result from photofragmentation of the heavier fragments or by increased fragmentation of the hfac ligand as the fluence is increased.

The implications of these observations are that the carbon and fluorine contamination observed in the films may result from photofragmentation of hfac after photodissociation from the palladium. The fragments are expected to be very reactive with hydrogen, and the products of the reactions will be volatile. Thus, in the gas-phase component of the deposition process, the presence of hydrogen will decrease the number of reactive species that can contaminate the surface and increase the number of saturated species that will be pumped away.

Summary

Metallic palladium films are produced by 308 nm laser-assisted chemical vapor deposition. X-ray photoelectron spectroscopic studies of the films produced with hydrogen as the carrier gas show a small carbon peak. X-ray diffraction shows that the films are polycrystalline fcc palladium with preferential growth along the 111 direction, and scanning electron microscopy shows that

(36) Mikami, N.; Ohki, R.; Kido, H. *Chem. Phys.* **1988**, *127*, 161.
(37) Mikami, N.; Ohki, R.; Kido, H. *Chem. Phys.* **1990**, *141*, 431.

the films formed with H_2 carrier gas consist of granules less than 35 nm in diameter. Luminescence is observed during the deposition process; peaks from palladium atoms dominate the luminescence, but peaks from CH and C_2 are also observed. Time-of-flight mass spectroscopy is used to further characterize the photofragments. The dominant peak in the mass spectrum is from palladium ions. No evidence for PdF or PdC is found (in contrast to the results from other metal hfac complexes where fluoride or carbide formation is common.) Carbon and fluorine contamination observed in the films probably results from photofragmentation of hfac after its photodissociation. In the gas-phase component of the deposition process, hydrogen carrier gas will react rapidly with these fragments and reduce the film contamination.

Acknowledgment. This work was made possible by a grant from the National Science Foundation (CHE 98-16552).

CM990566Q